J Math Chem (2012) 50:249–260
DOI 10.1007/s10910-011-9909-1

ORIGINAL PAPER

Superspherical-shape approximation to describe the morphology of small crystalline particles having near-polyhedral shapes with round edges

Tomotaka Miyazawa · Munehiro Aratake · Susumu Onaka

Received: 4 July 2011 / Accepted: 29 August 2011 / Published online: 18 September 2011

Abstract Small crystalline particles are often formed comprising near-polyhedral shapes with round edges. When near-polyhedral shapes are analyzed and discussed, it is convenient if these shapes can be expressed by equations with simple parameters. Superspheres are solids expressing various shapes between those of polyhedra and spheres. The superspherical-shape approximation is used in this study to consider the morphology of cubic crystal structure particles. Various near-polyhedral shapes composed of {100}, {111} and {110} planes are described using a simple equation with three shape-related parameters. It is shown that the superspherical-shape approximation is a useful geometrical tool for evaluating the morphology of small crystalline particles.

Keywords Particle · Surface energy · Equilibrium shape · Polyhedron · Supersphere

1 Introduction

Small crystalline particles are often formed comprising near-polyhedral shapes with round edges [1–5]. When near-polyhedral shapes are analyzed, it is convenient if these shapes can be expressed by equations with simple parameters. In 2001, Onaka considered the stress states of materials containing particles, and discussed the effect of particle shape when shapes are between those of cubes and spheres [6]. Onaka et al. used an equation for superspheres to describe intermediate shapes [6–9]. Onaka recently extended this equation for superspheres, and derived basic equations to describe shapes intermediate of various convex polyhedra and spheres [10,11]. In the present paper,

T. Miyazawa · M. Aratake · S. Onaka (✉)
Department of Materials Science and Engineering, Tokyo Institute of Technology,
4259-J2-63 Nagatsuta, Yokohama 226-8502, Japan
e-mail: onaka.s.aa@iem.titech.ac.jp

superspheres refer to intermediate shapes described by these basic equations [10]. The near-polyhedral shapes of small metal particles are discussed by approximating their shapes with superspheres.

For cubic crystal structure metals, the low-index {100}, {111} and {110} planes have lower values of surface-energy density. Near-polyhedral shapes composed of low-index planes are often observed for metal particles. The origin for this has been discussed with regards to the anisotropy of surface energy [1–5]. The quantitative evaluation of particle shapes is the basis of such discussion. In the present study, it is shown that the superspherical-shape approximation is a useful geometrical tool for describing the near-polyhedral shapes of crystalline particles.

2 Superspheres giving {100} – {111} – {110} polyhedra

The characteristics and currently available equations for superspheres are first summarized [10]. Crystallographic indices of cubic crystals are used in the present study. A distinct characteristic of superspheres is that the combined shapes of polyhedra and superspheres can be described by combining the equations of each polyhedron [10,11]. Figure 1 shows a {100} – {111} – {110} polyhedron formed by the combination of a {100} cube, {111} octahedron and {110} rhombic dodecahedron, in which the innermost surfaces of the three polyhedra are retained to form the combined polyhedron. Equations describing the shapes of superspheres have been derived from the spherical coordinates [10]. A basic equation that provides the radial coordinate of the {100} – {111} – {110} polyhedron is given by [10]:

$$r = \frac{R}{\left[G_0(1,0,0) + \left(\sqrt{3}\alpha\right)^p G_{\mathrm{I}}(\gamma,\gamma,\gamma) + \left(\sqrt{2}\beta\right)^p G_{\mathrm{II}}(\kappa,\kappa,0)\right]^{1/p}}, \qquad (1)$$

where R is the size parameter, p is the shape parameter for determining supersphere polyhedrality (i.e. the degree to which the supersphere is a polyhedron), and α and β are shape parameters for determining the ratios of the {100}, {111} and {110} surfaces of the polyhedron. The functions $G_0(1,0,0)$, $G_{\mathrm{I}}(\gamma,\gamma,\gamma)$ and $G_{\mathrm{II}}(\kappa,\kappa,0)$ in Eq. (1) describe the cubic, octahedral and dodecahedral superspheres, respectively, whose explicit expressions are given in Appendix I. The shape of the {100} – {111} – {110} polyhedron shown in Fig. 1 consists of six square {100}, eight equilateral-triangular {111} and 12 square {110} planes. This shape is given by Eq. (1), where $\alpha = 1/\left(2\sqrt{2}-1\right) \approx 0.547$, $\beta = 1/\sqrt{2} \approx 0.707$ and $p \to \infty$. Figure 2a–c show the change in shape given by Eq. (1) with increasing values of p.

Figure 3 is a diagram showing the dependence of polyhedron shape on α and β, given by Eq. (1) where $p \to \infty$. In Fig. 3, the shape is determined by the location in the quadrilateral surrounded by the points P of $(\alpha, \beta) = (1/3,\ 0.5)$, Q of $(0.5,\ 0.5)$, R of $(1,\ 1)$ and S of $(2/3,\ 1)$. The insets in Fig. 3 show various shapes in and around the quadrilateral. The diagram is summarized as follows:

1. Three basic polyhedra
   (a) {100} cube on point P

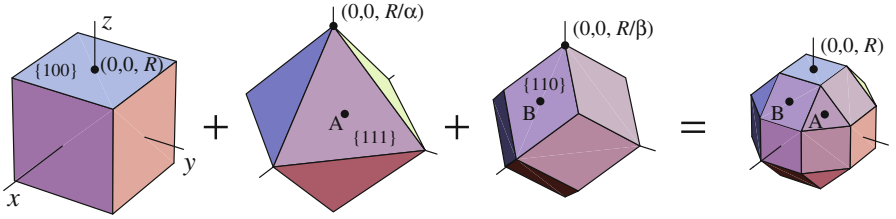

Fig. 1 The polyhedron afforded by the addition of a {100} cube, {111} octahedron and {110} dodecahedron. The resulting polyhedron is described by Eq. (1), where $p \to \infty$, $\alpha = 1/\left(2\sqrt{2}-1\right) \approx 0.547$ and $\beta = 1/\sqrt{2} \approx 0.707$. To illustrate the relationship between the polyhedra, the respective positions of octahedron point A and dodecahedron point B are indicated on the combined polyhedron

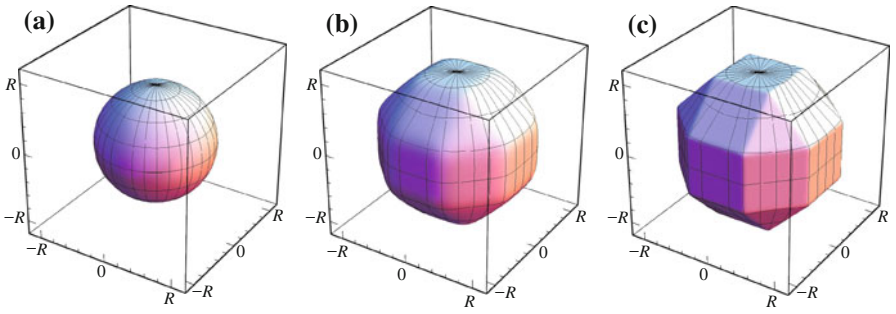

Fig. 2 Dependence of supersphere shape on the shape parameter p, as given by Eq. (1), where $\alpha = 1/\left(2\sqrt{2}-1\right) \approx 0.547$ and $\beta = 1/\sqrt{2} \approx 0.707$: **a** $p = 4$, **b** $p = 20$ and **c** $p = 100$

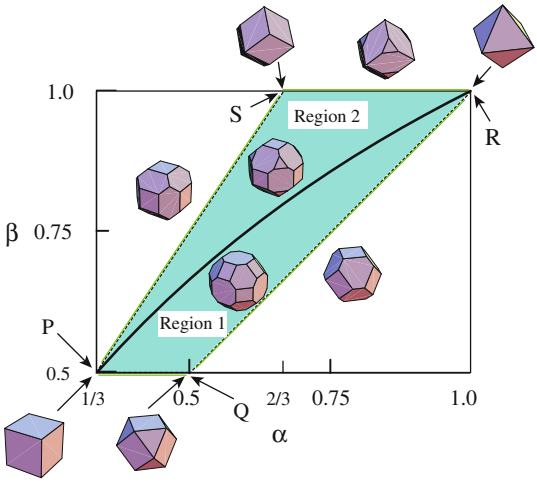

Fig. 3 Diagram showing the variation in shape of {100} – {111} – {110} polyhedra, given by Eq. (1) with $p \to \infty$

(b) {111} octahedron on point R
(c) {110} dodecahedron on point S

2. Combination of two basic polyhedra
   (a) {100} – {111} polyhedra changing from {100} cube to {111} octahedron on the line from P to R via Q, by truncating the eight vertices of the cube
   (b) {111} – {110} polyhedra changing from {111} octahedron to {110} dodecahedron on the line from R to S, by chamfering the 12 edges of the octahedron
   (c) {110} – {100} polyhedra changing from {110} dodecahedron to {100} cube on the line from S to P, by truncating six of the 14 vertices of the dodecahedron
3. Combination of three basic polyhedra
   (a) {100} – {111} – {110} polyhedra with mutually non-connected {110} surfaces in Region 1
   (b) {100} – {111} – {110} polyhedra with mutually connected {110} surfaces in Region 2

The boundary between Regions 1 and 2, expressed by the curve from P to R, is written as:

$$\beta = 2\alpha/(1+\alpha) \tag{2}$$

While the result presented in Fig. 3 has been previously demonstrated by Onaka [10], the boundary between Regions 1 and 2 in Fig. 3 is a new addition. The transition of polyhedra similar to that shown in Fig. 3 has recently been discussed by Suárez et al. [12]. In Appendix II, the volume and surface area of the polyhedra shown in Fig. 3 are written as a function of α and β.

3 Shape of small metal particles

The shapes of small metal particles shown in previous studies are now considered using the superspherical approximation. Menon and Martin reported producing ultrafine Ni particles by vapor condensation in an inert gas plasma reactor [5]. They reported the crystallographic characterization of the particles by transmission electron microscopy [5]. In Fig. 4, the inside curve shows the outline of a Ni particle observed from the $[1\bar{1}0]$ direction, which was traced from a micrograph shown in Fig. 5a of their paper [5]. The outside curve in Fig. 4 shows the outline of a supersphere with parameters $(\alpha,\ \beta,\ p) = (0.59,\ 0.63,\ 9.0)$ observed from the same direction. The inner and outer curves in Fig. 4 are in good agreement, with the supersphere well reproducing the near-polyhedral shape of the Ni particle.

Another example is shown in Fig. 5a and b, where the shape of an Al particle formed by evaporation [2] is compared with that of a supersphere. The inside curves in Fig. 5a and b show the outline of a single Al particle observed from the $[1\bar{1}0]$ and [100] directions, respectively. The Al particle shape when viewed from the two directions is shown in Figs. 2a and 3a of the original paper [2]. Comparing Figs. 5a and 4 in the current paper, it is clear that the Al particle has a greater degree of polyhedrality than the Ni particle. The outside curves in Fig. 5a and b are those of a supersphere with $(\alpha,\ \beta,\ p) = (0.60,\ 0.58,\ 14.4)$. Again, the supersphere well reproduces the

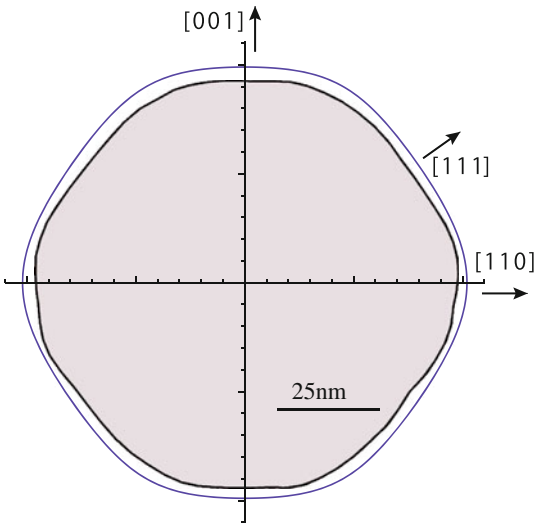

Fig. 4 The inside curve shows the outline of a Ni particle observed from the $[1\bar{1}0]$ direction, which was traced from a micrograph shown in Fig. 5a of the original paper [5]. The scale bar shows the size of the Ni particle. The outside curve is the outline of a supersphere with parameters $(\alpha,\ \beta,\ p) = (0.59,\ 0.63,\ 9.0)$ observed from the same direction

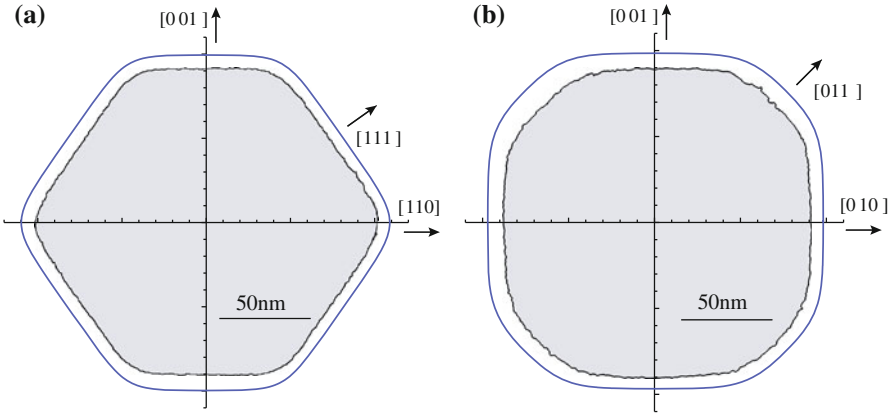

Fig. 5 The inside curves show the outlines of an Al particle observed from the **a** $[1\bar{1}0]$ and **b** [100] directions, which were traced from micrographs shown in Figs. 2a and 3a of the original paper [2]. The scale bars show the particle size. The outside curves in Figs. 4a and b are those of a supersphere with $(\alpha,\ \beta,\ p) = (0.60,\ 0.58,\ 14.4)$ observed from the same directions

near-polyhedral shape of the Al particle with a higher value of p. Kimoto and Nishida [2] describe the shape of the Al particle as a $\{100\}$ – $\{111\}$ polyhedron. However, Fig. 5a and b demonstrate that the $\{110\}$ surface also has a contribution to the particle shape.

4 Comparison with the Wulff shape

When the anisotropy of a material's surface-energy density is known, the Wulff shape provides an equilibrium shape determined by the surface energy [13,14]. In this

section, Wulff shapes are compared with superspherical shapes minimizing the surface energy. The anisotropy of surface-energy density treated here is based on the broken-bond model for face-centered-cubic (fcc) crystals [15].

The broken-bond model considers that the formation of surfaces in crystalline materials invariably results in the breaking of interatomic bonds across the surfaces [15]. In the nearest-neighbor broken-bond model for fcc crystals, the surface-energy density $\gamma_{\boldsymbol{h}}$ for a surface with a given unit normal vector $\boldsymbol{\nu}_{\boldsymbol{h}}$ is written as:

$$\gamma_{\boldsymbol{h}} = (\boldsymbol{\nu}_{\boldsymbol{h}} \cdot \boldsymbol{\nu}_{210})\, \gamma_{210}, \tag{3}$$

where γ_{210} and $\boldsymbol{\nu}_{210}$ are the maximum surface-energy density and unit normal vector for the {210} plane, respectively. The Wulff shape for the anisotropy of surface-energy density given by Eq. (3) is a {100} – {111} polyhedron with planar faces and sharp edges [5,11]. However, the shapes of small fcc metal particles usually have round edges, as is demonstrated in Figs. 4 and 5. This suggests that the anisotropy of real materials may be lower than that given by Eq. (3).

To change the degree of the anisotropy in Eq. (3), an index ϕ ($0 \leq \phi \leq 1$) is introduced, giving:

$$\gamma_{\boldsymbol{h}}/\gamma_{210} = (\boldsymbol{\nu}_{\boldsymbol{h}} \cdot \boldsymbol{\nu}_{210})^{\phi} \tag{4}$$

The anisotropy given by Eq. (4) decreases with decreasing ϕ over the range 1–0. While the introduction of ϕ is a phenomenological treatment, the anisotropy provided by the nearest-neighbor broken-bond model decreases when broken bonds between second or subsequent nearest neighbors are considered [5]. The contours of $\gamma_{\boldsymbol{h}}/\gamma_{210}$ provided by Eq. (4) and values for {100}, {111} and {110} surfaces for various values of ϕ are shown in Fig. 6.

The normalized surface energy N_Γ is given by:

$$N_\Gamma = \sum \gamma_{\boldsymbol{h}} ds \Big/ \left(\gamma_{210} V^{2/3}\right). \tag{5}$$

N_Γ is a measure of the shape's dependence on the surface energy, where ds is the surface element, and the summation of $\gamma_{\boldsymbol{h}} ds$ is made over the entire surface [11]. When ϕ is known, N_Γ of superspheres can be calculated using Eqs. (1), (4) and (5). The p dependence of N_Γ was first calculated and the minimum of N_Γ as a function of p was determined for the fixed values of α and β. Figure 7 shows the contours of the minimum N_Γ for $\phi = 0.5$ as a function of α and β. As shown in Fig. 7, the global minimum $N_{\Gamma(\min)}$ and shape parameters (α, β, p) providing the minimum are determined as $N_{\Gamma(\min)} = 4.642$ and (α, β, p) = (0.62, 0.66, 17.1). This analysis was carried out for various values of ϕ.

The Wulff shape can be determined as a function of ϕ, using the well-known method of construction [13,14]. Figure 8 shows a comparison between the shapes of superspheres giving the global minimum N_Γ (outside curves) and the Wulff shapes (inside curves) for (a) $\phi = 0.75$, (b) $\phi = 0.5$ and (c) $\phi = 0.25$. Figure 8 shows that the superspherical-shape approximation well reproduces the Wulff shapes even at low anisotropy of $\phi = 0.25$.

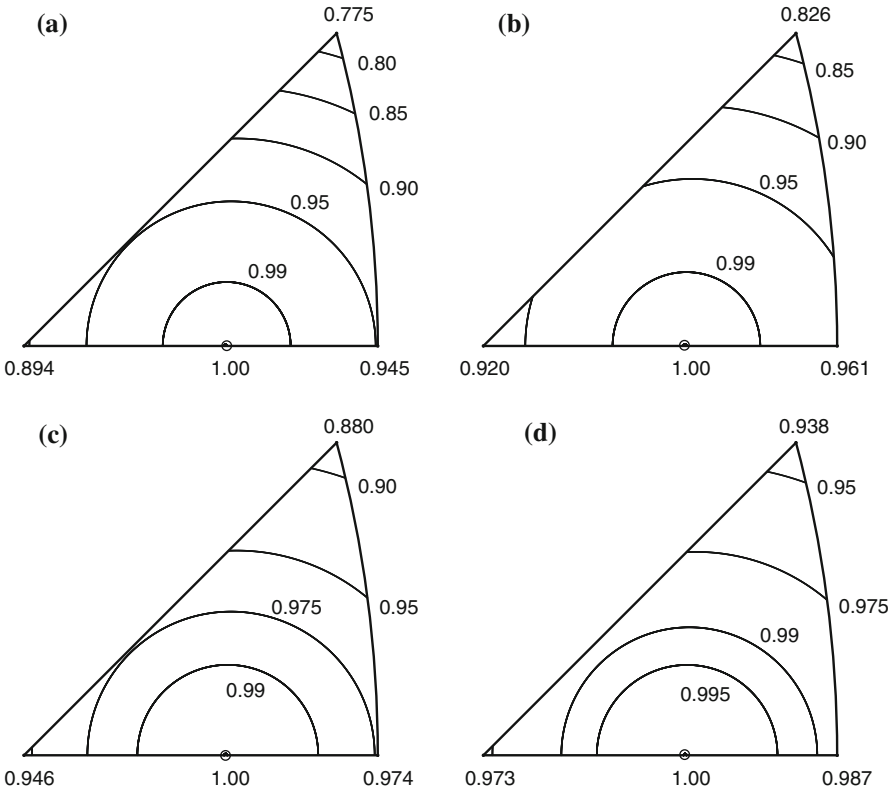

Fig. 6 Surface energy contours showing the values of γ_h/γ_{210} given by Eq. (4), for **a** $\phi = 1$ (the value for the nearest-neighbor broken-bond model), **b** $\phi = 0.75$, **c** $\phi = 0.5$ and **d** $\phi = 0.25$

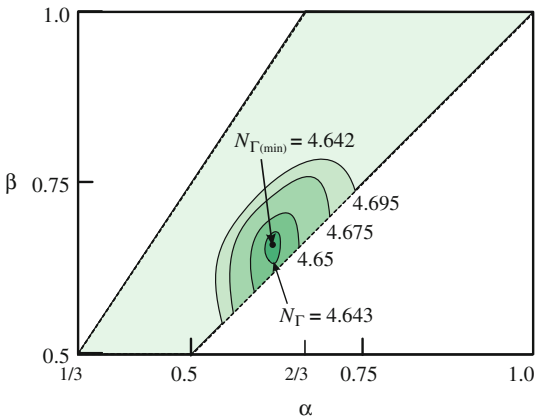

Fig. 7 The contours of the local minimum N_Γ as a function of α and β, for $\phi = 0.5$. The global minimum $N_{\Gamma(\min)}$ and shape parameters $(\alpha,\ \beta,\ p)$ providing the minimum are determined as $N_{\Gamma(\min)} = 4.642$ and $(\alpha,\ \beta,\ p) = (0.62,\ 0.66,\ 17.1)$

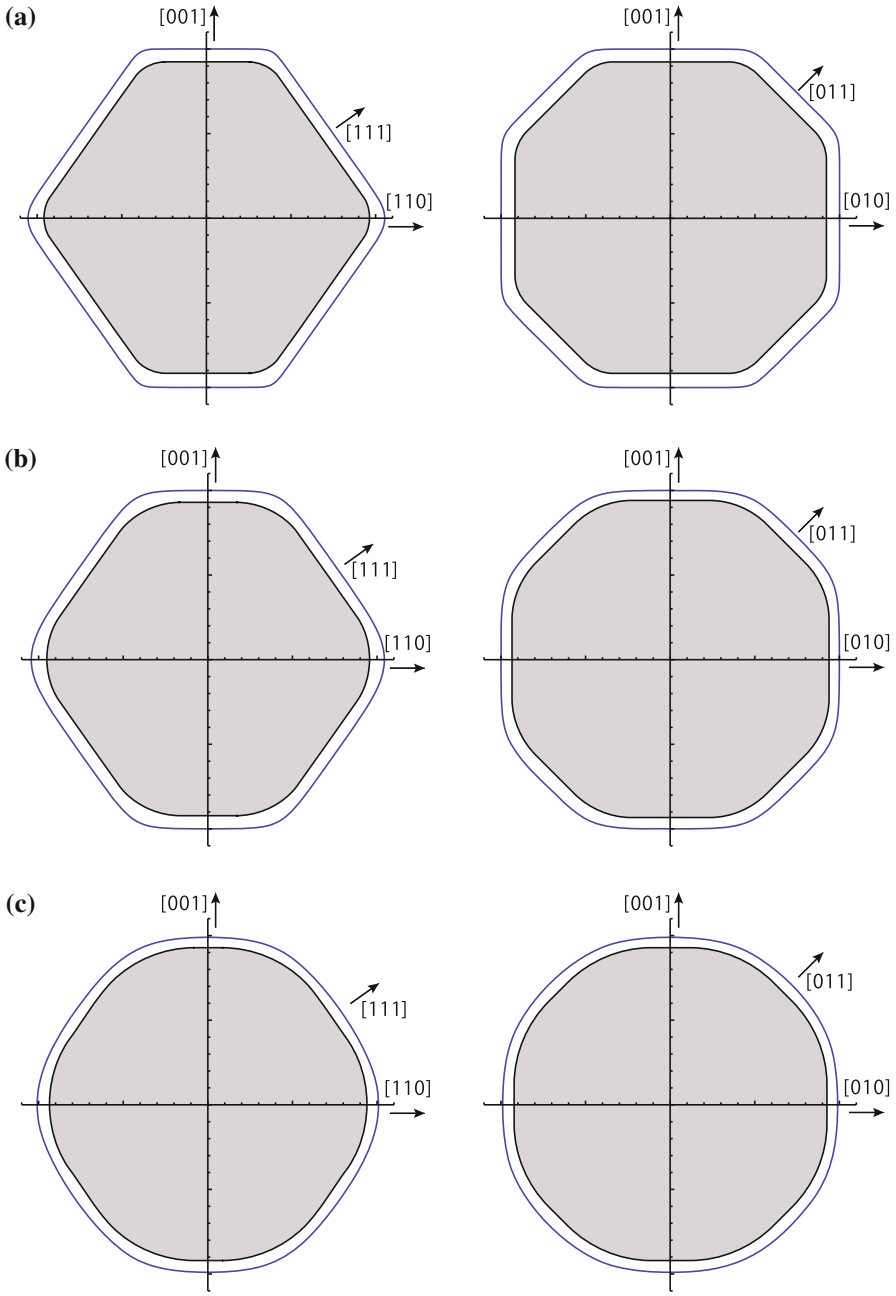

Fig. 8 Shapes of superspheres (*outside curves*) showing the global minimum N_Γ, and those of the Wulff shape (*inside curves*). View from the $[1\bar{1}0]$ (*left*) and [100] (*right*) directions for **a** $\phi = 0.75$, **b** $\phi = 0.5$ and **c** $\phi = 0.25$

Table 1 Shape parameters $(\alpha,\ \beta,\ p)$ of superspheres, showing the global minimum of N_Γ, $N_{\Gamma(\min)}$ for various values of the index ϕ

Index ϕ	Shape parameters giving $N_{\Gamma(\min)}$, $(\alpha,\ \beta,\ p)$	$N_{\Gamma(\min)}$
1	(2/3, 2/3, ∞) [5,11]	4.26 [11]
0.75	(0.64, 0.66, 39.4)	4.47
0.5	(0.62, 0.66, 17.1)	4.64
0.25	(0.59, 0.65, 9.4)	4.76

Values of the index ϕ, the global minimum N_Γ and shape parameters $(\alpha,\ \beta,\ p)$ providing the minimum are listed in Table 1. The results for $\phi = 1$ [5,11] of the nearest-neighbor broken-bond model are also included in Table 1. α and p decrease and the minimum N_Γ increases with decreasing ϕ.

The shape parameters $(\alpha,\ \beta,\ p) = (0.59,\ 0.63,\ 9.0)$ of the Ni particle shown in Fig. 4 are similar to values $(0.59,\ 0.65,\ 9.4)$ for $\phi = 0.25$ in Table 1. The shape parameters $(\alpha,\ \beta,\ p) = (0.60,\ 0.58,\ 14.4)$ of the Al particle shown in Fig. 5 are also similar to values $(0.62,\ 0.66,\ 17.1)$ for $\phi = 0.5$ in Table 1. While the reasons would be best discussed from a physical or chemical point of view, the present superspherical-shape approximation provides quantitative information for these similarities to be discussed. The anisotropy of surface energy or the energy criterion of the particle shape is often unknown, as is the case for the Ni and Al particles shown in Figs. 4 and 5, respectively. In such cases, the classification of particle shapes with simple parameters such as $(\alpha,\ \beta,\ p)$ is an effective method for discussing the origin of particle shapes. It is concluded that the superspherical-shape approximation is a useful geometrical tool for describing the near-polyhedral shapes of crystalline particles.

Acknowledgments This research was supported by a Grand-in-Aid for Scientific Research C (22560657) by the Japan Society for the Promotion of Science.

Appendix I

The functions $G_0(1,0,0)$, $G_{\rm I}(\gamma,\gamma,\gamma)$ and $G_{\rm II}(\kappa,\kappa,0)$ in Eq. (1)

When $p = 2$, the following equation using the $x - y - z$ orthogonal coordinate system gives a sphere with radius R:

$$|x/R|^p + |y/R|^p + |z/R|^p = 1\ (R > 0,\ \ p \geq 2). \tag{A1}$$

Alternatively, when $p \to \infty$ a cube with edges of $2R$ is given by Eq. (A1). Shapes intermediate of a sphere and cube are described by selecting an appropriate p value [6,10,11].

Equation (A1) is rewritten with the spherical coordinates (r, θ, φ) as [10]:

$$r_{\rm cube}(\theta,\varphi) = \frac{R}{[G_0(1,0,0)]^{1/p}}, \tag{A2a}$$

where

$$G_0(1,0,0) = |g(1,0,0)|^p + |g(0,1,0)|^p + |g(0,0,1)|^p \tag{A2b}$$

and

$$g\,(a,\ b,\ c) = a\,(\sin\theta\cos\varphi) + b\,(\sin\theta\sin\varphi) + c\,(\cos\theta)\,. \tag{A2c}$$

For an octahedral supersphere approaching a regular octahedron composed of {111} surfaces, the shape is given by [10]:

$$r_{\text{octa}}(\theta,\ \varphi) = \frac{R}{\left[\left(\sqrt{3}\alpha\right)^p G_{\text{I}}(\gamma,\gamma,\gamma)\right]^{1/p}}, \tag{A3a}$$

where

$$G_{\text{I}}(\gamma,\gamma,\gamma) = |g(\gamma,\gamma,\gamma)|^p + |g(-\gamma,\gamma,\gamma)|^p + |g(\gamma,-\gamma,\gamma)|^p + |g(\gamma,\gamma,-\gamma)|^p \tag{A3b}$$

and

$$\gamma = 1/\sqrt{3}. \tag{A3c}$$

As shown in Fig. 1, the parameter α determines the size of the octahedral supersphere and gives the coordinate of an octahedron vertex as $(0,\ 0,\ R/\alpha)$ when $p \to \infty$.

Alternatively, for a dodecahedral supersphere approaching a rhombic dodecahedron composed of {110} surfaces, the shape is given by [10]:

$$r_{\text{dodeca}}(\theta,\ \varphi) = \frac{R}{\left[\left(\sqrt{2}\beta\right)^p G_{\text{II}}(\kappa,\kappa,0)\right]^{1/p}}, \tag{A4a}$$

where

$$\begin{aligned} G_{\text{II}}(\kappa,\kappa,0) = {} & |g(\kappa,\kappa,0)|^p + |g(\kappa,-\kappa,0)|^p + |g(0,\kappa,\kappa)|^p \\ & + |g(0,\kappa,-\kappa)|^p + |g(\kappa,0,\kappa)|^p + |g(\kappa,0,-\kappa)|^p \end{aligned} \tag{A4b}$$

and

$$\kappa = 1/\sqrt{2}. \tag{A4c}$$

The parameter β also determines the size of the supersphere and gives the coordinate of a dodecahedron vertex as $(0,\ 0,\ R/\beta)$ when $p \to \infty$.

Appendix II

The volume and surface area of the polyhedra shown in Fig. 3

The volume V and the {100}, {111} and {110} surface area, S_{100}, S_{111} and S_{110} of the polyhedra shown in Fig. 3 are written as a function of α and β. In Region 1, these are given by

$$V = 4\left[\frac{1}{3\alpha^3}\left\{1-3\,(1-\alpha)^3\right\} - 2\left(\frac{1}{\alpha}-\frac{1}{\beta}\right)^2\left(3-\frac{1}{2\alpha}-\frac{1}{\beta}\right)\right]R^3,$$

$$S_{100} = 12\left\{\frac{1}{\alpha^2}\,(1-\alpha)^2 - 2\left(\frac{1}{\alpha}-\frac{1}{\beta}\right)^2\right\}R^2,$$

$$S_{111} = 4\sqrt{3}\left\{\left(3-\frac{1}{\alpha}\right)^2 - 3\left(2-\frac{1}{\beta}\right)^2\right\}R^2,$$

and

$$S_{110} = 24\sqrt{2}\left(\frac{1}{\alpha}-\frac{1}{\beta}\right)\left(2-\frac{1}{\beta}\right)R^2.$$

On the other hand, in Region 2, these are written as

$$V = 2\left\{\frac{1}{\beta^3} - \frac{1}{3}\left(\frac{3}{\beta}-\frac{2}{\alpha}\right)^3 - 4\left(\frac{1}{\beta}-1\right)^3\right\}R^3,$$

$$S_{100} = \frac{24}{\beta^2}\,(1-\beta)^2\,R^2,$$

$$S_{111} = 4\sqrt{3}\left(\frac{3}{\beta}-\frac{2}{\alpha}\right)^2 R^2,$$

and

$$S_{110} = 6\sqrt{2}\left\{\frac{1}{\beta^2} - \left(\frac{3}{\beta}-\frac{2}{\alpha}\right)^2 - 4\left(\frac{1}{\beta}-1\right)^2\right\}R^2.$$

The above results are valid for the polyhedron on the periphery of the quadrilateral PQRS. For example, when $(\alpha, \beta) = (1/3,\ 0.5)$, the above equations for Regions 1 and 2 commonly become

$$V = 8R^3,\ S_{100} = 24R^2 \text{ and } S_{111} = S_{110} = 0,$$

which are the results for the {100} cube with edges $2R$ on P. Among the various polyhedra in Fig. 3, the polyhedron having the minimum total surface area $S_{\mathrm{T}} = S_{100} + S_{110} + S_{111}$ under the same V is that of $\alpha = 1/\sqrt{3}$ and $\beta = 1/\sqrt{2}$ in Region

1, which has the normalized surface-area $N = S_T/V^{2/3} \approx 5.05$. This is the result obtained by Suárez et al. [16].

References

1. B.E. Sundquist, A direct determination of the anisotropy of the surface free energy of solid gold, silver, copper, nickel, and alpha and gamma iron. Acta Metall. **12**, 67–86 (1964)
2. K. Kimoto, I. Nishida, The crystal habits of small particles of aluminium and silver prepared by evaporation in clean atmosphere of argon. Jpn. J. Appl. Phys. **16**, 941–948 (1977)
3. J.C. Heyraud, J.J. Metois, Equilibrium shape of gold crystallites on a graphite cleavage surface: surface energies and interfacial energy. Acta Metall. **28**, 1789–1797 (1980)
4. J.C. Heyraud, J.J. Metois, Equilibrium shape and temperature. Surf. Sci. **128**, 334–342 (1983)
5. S.K. Menon, P.L. Martin, Determination of the anisotropy of surface free energy of fine metal particles. Ultramicroscopy **20**, 93–98 (1986)
6. S. Onaka, Averaged Eshelby tensor and elastic strain energy of a superspherical inclusion with uniform eigenstrains. Philos. Mag. Let. **81**, 265–272 (2001)
7. S. Onaka, N. Kobayashi, T. Fujii, M. Kato, Simplified energy analysis on the equilibrium shape of coherent γ' precipitates in γ matrix with a superspherical shape approximation. Intermetallics **10**, 343–346 (2002)
8. S. Onaka, N. Kobayashi, T. Fujii, M. Kato, Energy analysis with a superspherical shape approximation on the spherical to cubical shape transitions of coherent precipitates in materials with cubic structures. Mater. Sci. Eng. A. A **347**, 42–49 (2003)
9. S. Onaka, T. Fujii, M. Kato, Elastic strain energy due to misfit strains in a polyhedral precipitate composed of low-index planes. Acta Mater. **55**, 669–673 (2007)
10. S. Onaka, Simple equations giving shapes of various convex polyhedra: the regular polyhedra and polyhedra composed of crystallographically low-index planes. Philos. Mag. Lett. **86**, 175–183 (2006)
11. S. Onaka, Geometrical analysis of near polyhedral shapes with round edges in small crystalline particles or precipitates. J. Mater. Sci. **43**, 2680–2685 (2008)
12. J. Suárez, E. Gancedo, J. Manuel Álvarez, A. Morán, Truncating and chamfering diagrams of regular polyhedra. J. Math. Chem. **46**, 155–163 (2009)
13. C. Herring, Some theorems on the free energies of crystal surfaces. Phys. Rev. **82**, 87–93 (1951)
14. J.W. Cahn, C.A. Handwerker, Equilibrium geometries of anisotropic surfaces and interfaces. Mater. Sci. Eng. A. A **162**, 83–95 (1993)
15. J.K. Mackenzie, A.J.W. Moore, J.F. Nicholas, Bonds broken at atomically flat crystal surfaces-I. J. Phys. Chem. Solids **23**, 185–196 (1962)
16. J. Suárez, E. Gancedo, J. Manuel Álvarez, A. Morán, Optimum compactness structures derived from the regular octahedron. Eng. Struct. **30**, 3396–3398 (2008)